ARCHIVES OF ELECTRICAL ENGINEERING VOL. 63(3), pp. 489-506 (2014)

DOI 10.2478/aee-2014-0035

Influence of magnetic saturation effects on the fault detection of induction motors

PIOTR DROZDOWSKI, ARKADIUSZ DUDA

Cracow University of Technology
Faculty of Electrical and Computer Engineering
Institute of Electromechanical Energy Conversion
Warszawska 24, 31-155 Kraków, Poland
e-mail: {pdrozdow/aduda}@pk.edu.pk

(Received: 12.09.2013, revised: 27.03.2014)

Abstract: In this paper, the influence of impact damage to the induction motors on the zero-sequence voltage and its spectrum is presented. The signals detecting the damages result from a detailed analysis of the formula describing this voltage component which is induced in the stator windings due to core magnetic saturation and the discrete displacement of windings. Its course is affected by the operation of both the stator and the rotor. Other fault detection methods, are known and widely applied by analysing the spectrum of stator currents. The presented method may be a complement to other methods because of the ease of measurements of the zero voltage for star connected motors. Additionally, for converter fed motors the zero sequence voltage eliminates higher time harmonics displaced by 120 degrees. The results of the method application are presented through measurements and explained by the use of a mathematical model of the slip-ring induction motor.

Key words: induction motors, fault detection, saturation, zero sequence voltage

1. Introduction

The non-invasive methods of detection electrical and mechanical damages of induction motors are based mainly on the stator current spectrum analysis. The signals indicating various damages have been separated from the current spectrum during a long process of investigation by many researchers. One can mention several methods developed through mathematical modeling means [4, 12, 13, 15, 16] and the methods based on laboratory tests of various induction machines [1, 10] leading to a physical interpretation of obtained results. All the research studies have created a data-base that can be used for training the artificial intelligence detection systems [7].

The main subject of this paper is to reveal another damage information carrier signal. This is the zero sequence voltage, which is induced in the phase windings as a result of magnetic saturation [5, 10]. The waveform of this voltage depends on the state of the air-gap magnetic

field, where this field depends on the stator and rotor cooperation and also on the machine damages [9, 10]. The slip-ring induction motor was taken apart and the influence of the rotor circuit asymmetry was analyzed for investigation purposes. Results of laboratory tests have been interpreted with the use of a developed formula for the zero sequence voltage at steady state.

The research studies must answer the question if this method is promising for diagnostic purposes. As an object under investigation a low-power slip-ring induction motor was chosen. This is a specific machine that is different from cage motors with respect to the influence of harmonic fields and resulting detection signals. However, the assumed modeling method is common for both machine types and it has been trained using the slip ring motor where the stator and the rotor currents are available. The cage motors will be studied next.

The scheme of the laboratory stand is shown in Figure 1. The zero sequence voltage $u_s^{(0)} = 1/\sqrt{3}(u_U + u_V + u_W)$ results from the measured neutral voltage $u_n = 1/3(u_U + u_V + u_W)$ between the neutral point of the supplying transformer and the star point of the stator windings or the pseudo neutral point of resistors and the above star point. Therefore, $u_s^{(0)} = \sqrt{3}u_n$. The rotor circuit asymmetry has been introduced by opening the switch S for the breaking resistance R_{Mb} 500 times approximately greater than the rotor phase resistance.

To obtain the circuital model of the machine the phenomenon of magnetic saturation was modeled using a permeance function of the air-gap. The approach allows for approximating the air-gap magnetic flux density since the permeance function is strictly connected with the magneto motive force (MMF) exciting the field. The air gap non-uniformity (due to e.g. slotting) can be introduced as a signal modulating this permeance function. A similar approach was presented in [2], however it was presented for an eccentrically positioned rotor. This is simplification, however enabling self- and mutual inductances of the machine circuit that can be calculated using the formulae presented in [11] for electrical machines with a non-uniform air-gap. Thus, the machine voltage equations take the commonly known form

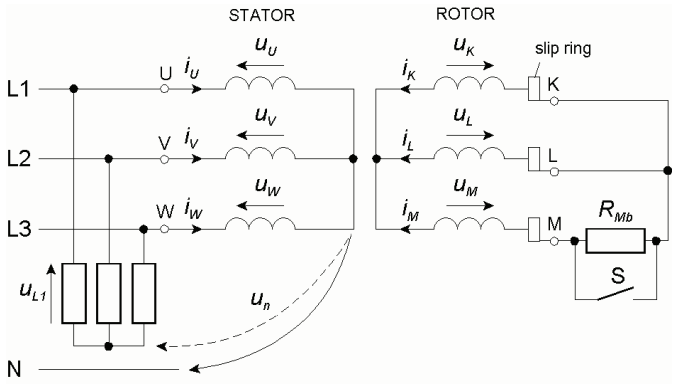

Fig. 1. Connection of the slip-ring induction motor for tests of rotor asymmetry

$$\mathbf{U} = \mathbf{R}\,\mathbf{I} + \mathbf{L}\frac{d}{dt}\mathbf{I} + \frac{d}{dt}\mathbf{M}\,\mathbf{I}, \tag{1}$$

where **R**, **L**, **M** are the matrices of resistances, leakage inductances and self- and mutual inductances, respectively. Vectors of voltages and currents are denoted by **U** and **I**, respecti-

vely. On the basis of this model the mathematical formulae can be developed and used for interpreting of measured signals.

2. Mathematical background for induction motor diagnostics

2.1. Main assumptions for the mathematical model

- Magnetic core is saturated only due to the first non-zero symmetrical components of stator and rotor currents. For the slip ring motors this is clear, however for the cage induction motors this is a simplification.
- The effect of saturation is simulated as enlarging the air-gap length at the location α_M, where the total MMF of the machine reaches a maximum with respect to the stator phase U assumed to be the first one. The MMF is represented by the magnetising current i_{M} to be defined below. This varying air-gap is expressed with the per unit permeance function approximated with harmonic series of the following form utilising the Euler's identity:

$$\Lambda_{\mathrm{sat}}^{\mathrm{pu}}(x,\alpha_M)=\sum_{\mu}\Lambda_{\mu}^{\mathrm{pu}}(i_M)\,e^{j\mu p(x-\alpha_M)};\ \mu=0,\pm2,\pm6,\pm10,\pm14,... \tag{2}$$

The base permeance:

$$\Lambda_{\mathrm{B}}=\frac{2\mu_o r_c l_c}{\pi p^2\delta},$$

where $\mu_o=4\pi\cdot10^{-7}$ H/m, r_c – inside stator radius, l_c – equivalent length of the machine core, δ – air-gap equivalent length comprising the Carter's factor k_C, p – pole pair number of the machine, x – angle along the air-gap of the machine cross section with respect to the phase U.

The coefficients of the series (2) are given by the following expressions

$$\Lambda_0^{\mathrm{pu}}=\frac{1}{k_{\mathrm{sat}}},\quad \Lambda_{\mu}^{\mathrm{pu}}=(-1)^{\mu/2}\frac{\exp(1-\frac{\mu}{2})}{2p}\Lambda_0^{pu}\left(\Lambda_0^{pu}-1\right)_{|\mu=2,6,10,...} \tag{3}$$

where the saturation factor can be approximated by the function

$$k_{\mathrm{sat}}=\frac{c\,i_M^{pu}+\varepsilon}{\operatorname{arc\,tg}(c\,i_M^{pu})+\varepsilon};\ \varepsilon<<1$$

resulting from the magnetisation curve calculated as

$$\Psi^{pu}=\operatorname{arc\,tg}(c\,i_M^{pu})/\operatorname{arc\,tg}(c).$$

- The effect of slotting is modelled as a modulating signal f_{slo} for the previously defined permeance (2)

$$f_{\mathrm{slo}}(x,\varphi)=\sum_{k,l}A_k B_l\,e^{j(kZ_s+lZ_r)x}e^{-jlZ_r\varphi}. \tag{4}$$

In the above: Z_s – number of stator slots, Z_r – number of rotor slots,

$$k = 0, \pm 1, \pm 2, \ldots; \; l = 0, \pm 1, \pm 2, \ldots \quad A_k = (-1)^k a_k^{\mathrm{sgn}|k|}, \; B_l = (-1)^l b_k^{\mathrm{sgn}|l|},$$

$$a_k \approx \frac{k_{Cs}}{\pi(|k|+\varepsilon)}\beta_s, \quad b_l \approx \frac{k_{Cr}}{\pi(|l|+\varepsilon)}\beta_r, .$$

According to [6, 8],

$$\beta_{s,r} = \frac{0.8\dfrac{b_o^{s,r}}{\delta_o}}{\dfrac{b_o^{s,r}}{\delta_o}+9},$$

where $b_o^{s,r}$ – stator or rotor slot opening, δ_o – geometrical air-gap length, k_{Cs}, k_{Cr} – Carter's factors for the stator and the rotor respectively, $k_C = k_{Cs}k_{Cr}$ – machine Carter's factor.

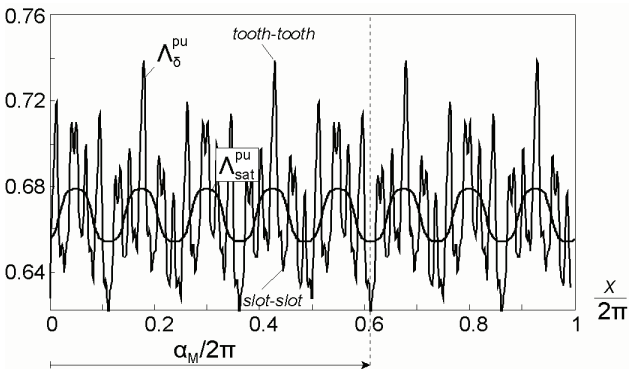

Fig. 2. Distribution of the permeance function

- The air-gap permeance
  Modulating (2) with (4) gives

$$\Lambda_\delta^{pu}(x,\alpha_M,\varphi,i_M) = f_{slo}(x,\varphi)\Lambda_{sat}^{pu}(x,\alpha_M,i_M) = \\ = \sum_{k,l} A_k B_l e^{j(kZ_z+lZ_r)x} e^{jlZ_r\varphi} \sum_\mu \Lambda_\mu^{pu}(i_M) e^{j\mu p(x-\alpha_M)}. \tag{5}$$

The examplary distribution of the permeance function (5) is shown in Figure 2 for $Z_s = 36$, $Z_r = 24$, $p = 4$ and the saturation factor $k_{sat} = 1.5$.

- The new harmonic orders can be defined now by creating the harmonic sets:

$$\left.\begin{aligned} H_\mu &= \{\mu = 2i \,;\; i = 0, \pm 1, \pm 3, \pm 5, \ldots\} \\ H_m &= \{m = kZ_s + lZ_r + \mu p \,;\; k = 0, \pm 1, \pm 2, \ldots \,;\; l = 0, \pm 1, \pm 2, \ldots\} \\ H_n &= \{n = -lZ_r \,;\; l = 0, \pm 1, \pm 2, \ldots\} \end{aligned}\right\}. \tag{6}$$

- The function of the air-gap permeance takes the generic form:

$$\Lambda_{\delta}^{\mathrm{pu}}(x,\alpha,\varphi,i_M)=\sum_{\mu\in H_\mu,m\in H_m,n\in H_n}\Lambda_{m,n}^{\mathrm{pu}}(i_M)e^{-j\mu\alpha}e^{jmx}e^{jn\varphi}, \tag{7}$$

$$\alpha=p\alpha_M. \tag{8}$$

The permeance coefficient $\Lambda_{m,n}^{\mathrm{pu}}(i_M)$ depends on the harmonic number μ, that is "hidden" now in the index m. For the machine without slotting $m=\mu p$ and $n=0$.

- The winding inductances are calculated using the formulae defined in [11] for the machine with a non-uniform air-gap. The machine model is formulated as a connection of resistances and inductances. Hence, the mutual inductance of the two windings a and b, positioned with respect to the stator at the locations x_a and x_b, respectively, is given by the function:

$$M_{ab}^{s/r/sr}=\sum_{\mu\in H_\mu}\sum_{\nu\in H_\nu}\sum_{m\in H_m}\sum_{n\in H_n}M_{\nu,m}^{s/r/sr}e^{-j\mu\alpha}e^{-j\nu x_a}e^{j(\nu+m)x_b}e^{jn\varphi}, \tag{9}$$

where

$$\left.\begin{array}{c}\forall\,\nu\in H_\nu\wedge\forall m\in H_m\Rightarrow\rho=-(\nu+m)\in H_\rho\\ \Downarrow\\ M_{\nu,m}^{s/r/sr}=\dfrac{N_a k_a^{|\nu|}N_b k_b^{|\nu+m|}}{|\nu||\nu+m|}\Lambda_{\mathrm{B}}\Lambda_{m,n}^{\mathrm{pu}}(i_M)\end{array}\right\}, \tag{10}$$

where: N_a, N_b – turn numbers of the windings a and b, respectively, $k_a^{|\nu|}$, $k_b^{|\nu+m|}$ – the winding factors for the respective harmonics ν and $\nu+m$. For the machine with a "smooth" air-gap the formula for the mutual inductance of windings a and b resulting from (10), takes the well known form.

The mutual inductance (10) exists when the following condition is satisfied for the assumed harmonic orders $\nu\in H_\nu$, $\rho\in H_\rho$, $m\in H_m$:

$$\nu+\rho+m=0. \tag{11}$$

This equation assures the harmonic balance inside the mathematical model and must be satisfied for sets of harmonic orders. Therefore, the assumption for the set contents influences the accuracy of the mathematical model.

For symmetrically designed windings the MMF harmonics have the orders belonging to the sets:

$$H_\nu=\{(2i_1-1)p;\,i_1=0,\pm1,\pm2,\ldots\} \tag{12}$$

for the winding a and

$$H_\rho=\{(2i_2-1)p;\,i_2=0,\pm1,\pm2,\ldots\} \tag{13}$$

for the winding b.

The phase winding positions for the 3-phase slip-ring induction motor are given below:
– for the stator

$$x_a = (a-1)\beta_s;\ x_b = (b-1)\beta_s;$$
$$a = 1, 2, 3;\ b = 1, 2, 3;\ \beta_s = \frac{2\pi}{3p}, \tag{14}$$

– for the rotor

$$x_a = (a-1)\beta_r + \varphi;\ x_b = (b-1)\beta_r + \varphi;$$
$$a = 1, 2, 3;\ b = 1, 2, 3;\ \beta_r = \frac{2\pi}{3p}, \tag{15}$$

where: φ – rotor rotation angle.

2.2. Voltage equations of the motor in machine variables

The machine voltage equations are transformed from the natural system to symmetrical components. This transformation splits the harmonic components of inductances assigning them to voltage equations accompanying the respective symmetrical components.
The voltage equations of the motor in machine variables can be shown in the matrix form:

$$\begin{bmatrix} \mathbf{u}_\mathbf{s}^\mathbf{I} \\ \mathbf{u}_\mathbf{r}^\mathbf{I} \end{bmatrix} = \begin{bmatrix} \mathbf{R}_\mathbf{s}^\mathbf{I} & \\ & \mathbf{R}_\mathbf{r}^\mathbf{I} \end{bmatrix} \begin{bmatrix} \mathbf{i}_\mathbf{s}^\mathbf{I} \\ \mathbf{i}_\mathbf{r}^\mathbf{I} \end{bmatrix} + \begin{bmatrix} \mathbf{L}_\mathbf{sl}^\mathbf{I} & \\ & \mathbf{L}_\mathbf{rl}^\mathbf{I} \end{bmatrix} \frac{\mathrm{d}}{\mathrm{d}t} \begin{bmatrix} \mathbf{i}_\mathbf{s}^\mathbf{I} \\ \mathbf{i}_\mathbf{r}^\mathbf{I} \end{bmatrix} + \frac{\mathrm{d}}{\mathrm{d}t} \begin{bmatrix} \mathbf{M}_\mathbf{s}^\mathbf{I} & \mathbf{M}_\mathbf{sr}^\mathbf{I} \\ \mathbf{M}_\mathbf{rs}^\mathbf{I} & \mathbf{M}_\mathbf{r}^\mathbf{I} \end{bmatrix} \begin{bmatrix} \mathbf{i}_\mathbf{s}^\mathbf{I} \\ \mathbf{i}_\mathbf{r}^\mathbf{I} \end{bmatrix} \tag{16}$$

or separately for the stator and the rotor

$$\begin{bmatrix} u_{s1} \\ u_{s2} \\ u_{s3} \end{bmatrix} = \begin{bmatrix} R_{s1} & & \\ & R_{s2} & \\ & & R_{s3} \end{bmatrix} \begin{bmatrix} i_{s1} \\ i_{s2} \\ i_{s3} \end{bmatrix} + \begin{bmatrix} L_{s1} & & \\ & L_{s2} & \\ & & L_{s3} \end{bmatrix} \frac{\mathrm{d}}{\mathrm{d}t} \begin{bmatrix} i_{s1} \\ i_{s2} \\ i_{s3} \end{bmatrix} + \frac{\mathrm{d}}{\mathrm{d}t} \mathbf{M}_\mathbf{s}^\mathbf{I} \begin{bmatrix} i_{s1} \\ i_{s2} \\ i_{s3} \end{bmatrix} + \frac{\mathrm{d}}{\mathrm{d}t} \mathbf{M}_\mathbf{sr}^\mathbf{I} \begin{bmatrix} i_{r1} \\ i_{r2} \\ i_{r3} \end{bmatrix} \tag{17}$$

$\mathbf{u}_\mathbf{s}^\mathbf{I}$ $\mathbf{R}_\mathbf{s}^\mathbf{I}$ $\mathbf{i}_\mathbf{s}^\mathbf{I}$ $\mathbf{L}_\mathbf{sl}^\mathbf{I}$

$$\begin{bmatrix} u_{r1} \\ u_{r2} \\ u_{r3} \end{bmatrix} = \begin{bmatrix} R_{r1} & & \\ & R_{r2} & \\ & & R_{r3} \end{bmatrix} \begin{bmatrix} i_{r1} \\ i_{r2} \\ i_{r3} \end{bmatrix} + \begin{bmatrix} L_{r1} & & \\ & L_{r2} & \\ & & L_{r3} \end{bmatrix} \frac{\mathrm{d}}{\mathrm{d}t} \begin{bmatrix} i_{r1} \\ i_{r2} \\ i_{r3} \end{bmatrix} + \frac{\mathrm{d}}{\mathrm{d}t} \mathbf{M}_\mathbf{r}^\mathbf{I} \begin{bmatrix} i_{r1} \\ i_{r2} \\ i_{r3} \end{bmatrix} + \frac{\mathrm{d}}{\mathrm{d}t} \mathbf{M}_\mathbf{sr}^{\mathbf{I}\,T} \begin{bmatrix} i_{s1} \\ i_{s2} \\ i_{s3} \end{bmatrix}, \tag{18}$$

$\mathbf{u}_\mathbf{r}^\mathbf{I}$ $\mathbf{R}_\mathbf{r}^\mathbf{I}$ $\mathbf{i}_\mathbf{r}^\mathbf{I}$ $\mathbf{L}_\mathbf{rl}^\mathbf{I}$

where the superscript T denotes matrix transposition.

Vectors of voltages and currents contain: $u_{s1} = u_U$, $u_{s2} = u_V$, $u_{s3} = u_W$ – stator phase winding voltages, $i_{s1} = i_U$, $i_{s2} = i_V$, $i_{s3} = i_W$ – stator phase currents, $u_{r1} = u_K$, $u_{r2} = u_L$, $u_{r3} = u_M$ – rotor phase voltages, $i_{r1} = i_K$, $i_{r2} = i_L$, $i_{r3} = i_M$ – rotor phase currents.

The matrices of resistances and leakage inductances are diagonal with generally different elements Z_{x1}, Z_{x2}, Z_{x3} for each phase winding, where the substitution $Z = R$ or $Z = L$ and $x = s$ for the stator and $x = r$ for the rotor must be performed. The matrices of self- and mutual inductances have the forms resulting directly from (8) for the position angles (13) and (14).

Inductance matrices

$$\mathbf{M}_\mathbf{s}^\mathbf{I} = \sum_{\mu \in H_\mu} \sum_{\nu \in H_\nu} \sum_{m \in H_m} \sum_{n \in H_n} M_{\nu,m}^s e^{-j\mu\alpha} e^{jn\varphi} \begin{bmatrix} 1 \\ e^{-j\nu\beta_s} \\ e^{-j\nu 2\beta_s} \end{bmatrix} \begin{bmatrix} 1 & e^{j(\nu+m)\beta_s} & e^{j(\nu+m)2\beta_s} \end{bmatrix}, \tag{19}$$

$$\mathbf{M}_{\mathbf{r}}^{\mathbf{I}} = \sum_{\mu\in H_\mu}\sum_{\nu\in H_\nu}\sum_{m\in H_m}\sum_{n\in H_n} M_{\nu,m}^{r} e^{-j\mu\alpha} e^{j(m+n)\varphi} \begin{bmatrix} 1 \\ e^{-j\nu\beta_r} \\ e^{-j\nu 2\beta_r} \end{bmatrix} \begin{bmatrix} 1 & e^{j(\nu+m)\beta_r} & e^{j(\nu+m)2\beta_r} \end{bmatrix}, \tag{20}$$

$$\mathbf{M}_{\mathbf{sr}}^{\mathbf{I}} = \sum_{\mu\in H_\mu}\sum_{\nu\in H_\nu}\sum_{m\in H_m}\sum_{n\in H_n} M_{\nu,m}^{sr} e^{-j\mu\alpha} e^{j(\nu+m+n)\varphi} \begin{bmatrix} 1 \\ e^{-j\nu\beta_s} \\ e^{-j\nu 2\beta_s} \end{bmatrix} \begin{bmatrix} 1 & e^{j(\nu+m)\beta_r} & e^{j(\nu+m)2\beta_r} \end{bmatrix}. \tag{21}$$

2.3. Description in symmetrical components

Transformation voltages, currents and fluxes into symmetrical components can be performed using the matrix $\mathbf{S_s}$ for the stator and $\mathbf{S_r}$ for the rotor, respectively. These matrices are given below.

$$\mathbf{S_s} = \frac{1}{\sqrt{3}} \begin{bmatrix} 1 & 1 & 1 \\ 1 & \underline{a} & \underline{a}^2 \\ 1 & \underline{a}^2 & \underline{a} \end{bmatrix}; \underline{a} = e^{j2\pi/3} = e^{jp\beta_s}, \tag{22}$$

$$\mathbf{S_r} = \frac{1}{\sqrt{3}} \begin{bmatrix} 1 & & \\ & e^{jp\varphi} & \\ & & e^{-jp\varphi} \end{bmatrix} \begin{bmatrix} 1 & 1 & 1 \\ 1 & \underline{a} & \underline{a}^2 \\ 1 & \underline{a}^2 & \underline{a} \end{bmatrix}; \underline{a} = e^{j2\pi/3} = e^{jp\beta_r}. \tag{23}$$

After the transformation the structure of equations remains the same as (12) with the superscript **II** indicating the vectors and matrices that now are described with complex numbers:

$$\begin{bmatrix} u_s^{(0)} \\ \underline{u}_s^{(1)} \\ \underline{u}_s^{(2)} \end{bmatrix} = \mathbf{R_s^{II}} \begin{bmatrix} i_s^{(0)} \\ \underline{i}_s^{(1)} \\ \underline{i}_s^{(2)} \end{bmatrix} + \mathbf{L_{sl}^{II}} \frac{\mathrm{d}}{\mathrm{d}t} \begin{bmatrix} i_s^{(0)} \\ \underline{i}_s^{(1)} \\ \underline{i}_s^{(2)} \end{bmatrix} + \frac{\mathrm{d}}{\mathrm{d}t} \mathbf{M_s^{II}} \begin{bmatrix} i_s^{(0)} \\ \underline{i}_s^{(1)} \\ \underline{i}_s^{(2)} \end{bmatrix} + \frac{\mathrm{d}}{\mathrm{d}t} \mathbf{M_{sr}^{II}} \begin{bmatrix} 0 \\ \underline{i}_r^{(1)} \\ \underline{i}_r^{(2)} \end{bmatrix} \tag{24}$$

$\mathbf{u_s^{II}}$ $\mathbf{i_s^{II}}$ $\mathbf{i_r^{II}}$

$$\begin{bmatrix} u_r^{(0)} \\ \underline{u}_r^{(1)} \\ \underline{u}_r^{(2)} \end{bmatrix} = \mathbf{u_r^{II}} = \mathbf{R_r^{II}}\mathbf{i_r^{II}} + \mathbf{L_{rl}^{II}}\frac{\mathrm{d}}{\mathrm{d}t}\mathbf{i_r^{II}} + \frac{\mathrm{d}}{\mathrm{d}t}\mathbf{M_r^{II}}\mathbf{i_r^{II}} + \frac{\mathrm{d}}{\mathrm{d}t}\mathbf{M_{sr}^{II*}}\mathbf{i_s^{II}} - \tag{25}$$

$$- jp\frac{\mathrm{d}\varphi}{\mathrm{d}t}\left\{\left(\mathbf{L_{rl}^{II}} + \mathbf{M_r^{II}}\right)\mathbf{i_r^{II}} + \mathbf{M_{sr}^{II*}}\mathbf{i_s^{II}}\right\}.$$

In the above equations: $\underline{u}_s^{(2)} = \underline{u}_s^{(1)*}$, $\underline{u}_r^{(2)} = \underline{u}_r^{(1)*}$, $\underline{i}_s^{(2)} = \underline{i}_s^{(1)*}$, $\underline{i}_r^{(2)} = \underline{i}_r^{(1)*}$.

The symmetrical components are vectors in the stationary reference frame α-β. The real and imaginary parts are denoted by α and β, respectively. Additionally: $\underline{x}^*$ – complex conjugate of $\underline{x}$.

The resistance matrices $\mathbf{R_s^{II}}$, $\mathbf{R_r^{II}}$ and the leakage inductances $\mathbf{L_{sl}^{II}}$, $\mathbf{L_{rl}^{II}}$ have the same generic structure:

$$\mathbf{Z_x^{II}} = \begin{bmatrix} 1 & & \\ & e^{j\Phi} & \\ & & e^{-j\Phi} \end{bmatrix} \begin{bmatrix} Z_{x0} & \underline{Z}_x^* & \underline{Z}_x \\ \underline{Z}_x & Z_{x0} & \underline{Z}_x^* \\ \underline{Z}_x^* & \underline{Z}_x & Z_{x0} \end{bmatrix} \begin{bmatrix} 1 & & \\ & e^{-j\Phi} & \\ & & e^{j\Phi} \end{bmatrix}$$

$$\begin{aligned} &Z_0 = Z_{x1} + Z_{x2} + Z_{x3} \\ &\underline{Z} = Z_{x1} + \underline{a} Z_{x2} + \underline{a}^2 Z_{x3} \\ &\underline{Z} = R \text{ or } \underline{L} \;\; ; \;\; x = s \text{ or } r \text{ or } sl \text{ or } rl \end{aligned} \tag{26}$$

$$\Phi = 0 \text{ for } x = s, \Phi = p\varphi \text{ for } x = r.$$

The matrices of self and mutual inductances have the following structures:

$$\mathbf{M_s^{II}} = 3 \sum_{\mu \in H_\mu} \sum_{\nu \in H_\nu} \sum_{m \in H_m} \sum_{n \in H_n} M_{\nu,m}^{s} \; e^{-j\mu\alpha} e^{jn\varphi} \mathbf{Q_s}, \tag{27}$$

$$\begin{aligned} \mathbf{M_r^{II}} = 3 &\sum_{\mu \in H_\mu} \sum_{\nu \in H_\nu} \sum_{m \in H_m} \sum_{n \in H_n} M_{\nu,m}^{r} \; e^{-j\mu\alpha} e^{j(m+n)\varphi} \cdot \\ &\cdot \operatorname{diag}[1, e^{jp\varphi}, e^{-jp\varphi}] \, \mathbf{Q_r} \, \operatorname{diag}[1, e^{-jp\varphi}, e^{jp\varphi}], \end{aligned} \tag{28}$$

$$\mathbf{M_{sr}^{II}} = 3 \sum_{\mu \in H_\mu} \sum_{\nu \in H_\nu} \sum_{m \in H_m} \sum_{n \in H_n} M_{\nu,m}^{sr} \; e^{-j\mu\alpha} e^{j(\nu+m+n)\varphi} \mathbf{Q_{sr}} \operatorname{diag}[1, e^{-jp\varphi}, e^{jp\varphi}], \tag{29}$$

3×3 matrices $\mathbf{Q_s}$, $\mathbf{Q_r}$, $\mathbf{Q_{sr}}$ have their elements $Q_{s/r/sr}$ equal to 1 or 0. The element $Q_{s/r/sr} = 1$ if for the given harmonic orders $\nu \in H_\nu$, associated with the row, and $\rho \in H_\rho$, associated with the column, the condition for the harmonic order $m = -\nu - \rho \in H_m$ is satisfied. This harmonic condition is indicated by the subscript 1 in the matrix structure. Thus, the generic form is

$$\mathbf{Q_{s/r/sr}} = \begin{bmatrix} 1_{m=-\nu^{(0)}-\rho^{(0)} \in H_m} & 1_{m=-\nu^{(0)}-\rho^{(1)} \in H_m} & 1_{m=-\nu^{(0)}-\rho^{(2)} \in H_m} \\ 1_{m=-\nu^{(1)}-\rho^{(0)} \in H_m} & 1_{m=-\nu^{(1)}-\rho^{(1)} \in H_m} & 1_{m=-\nu^{(1)}-\rho^{(2)} \in H_m} \\ 1_{m=-\nu^{(2)}-\rho^{(0)} \in H_m} & 1_{m=-\nu^{(2)}-\rho^{(1)} \in H_m} & 1_{m=-\nu^{(2)}-\rho^{(2)} \in H_m} \end{bmatrix} \begin{matrix} \nu^{(0)}=(3+6k_1)p \\ \nu^{(1)}=(1+6k_2)p \\ \nu^{(2)}=-(1+6k_2)p \end{matrix} \Bigg\} \in H_\nu \quad k_1=\ldots,-2,-1,0,1,\ldots \; k_2=\ldots,-1,0,1,\ldots$$

$$\rho^{(0)}=-(3+6l_1)p \qquad \rho^{(1)}=-(1+6l_2)p \qquad \rho^{(2)}=(1+6l_2)p \quad \in H_\rho \; ; l_1=\ldots,-2,-1,0,1,\ldots; \; l_2=\ldots,-1,0,1,\ldots \tag{30}$$

The electromagnetic torque takes the form:

$$T_e = \frac{\partial}{\partial \varphi} \frac{1}{2} \begin{bmatrix} \mathbf{i_s^{II*}} & \mathbf{i_r^{II*}} \end{bmatrix} \begin{bmatrix} \mathbf{M_s^{II}} & \mathbf{M_{sr}^{II}} \\ \mathbf{M_{sr}^{II*}} & \mathbf{M_r^{II}} \end{bmatrix} \begin{bmatrix} \mathbf{i_s^{II}} \\ \mathbf{i_r^{II}} \end{bmatrix}; \qquad \begin{aligned} \mathbf{i_s^{II}} &= \begin{bmatrix} i_s^{(0)} & \underline{i}_s^{(1)} & \underline{i}_s^{(2)} \end{bmatrix}^T \\ \mathbf{i_r^{II}} &= \begin{bmatrix} i_r^{(0)} & \underline{i}_r^{(1)} & \underline{i}_r^{(2)} \end{bmatrix}^T \end{aligned} . \tag{31}$$

Parameters of the magnetising current vector are described according to the formulae given below.

$$i_M = \sqrt{i_{M\alpha}^2 + i_{M\beta}^2}, \tag{32}$$

$$i_{M\alpha} = \tfrac{1}{\sqrt{3}} (i_{s1} - \tfrac{1}{2} i_{s2} - \tfrac{1}{2} i_{s3}) + \tfrac{1}{n_{sr}} \left[\tfrac{\sqrt{3}}{2} i_{r1} \cos p\varphi - \tfrac{1}{2} (i_{r2} - i_{r3}) \sin p\varphi \right], \tag{33}$$

$$i_{M\beta} = \tfrac{1}{2}(i_{s2} - i_{s3}) + \tfrac{1}{n_{sr}}\left[\tfrac{\sqrt{3}}{2} i_{r1} \sin p\varphi + \tfrac{1}{2}(i_{r2} - i_{r3}) \cos p\varphi\right], \tag{34}$$

$$\alpha = \operatorname{arctg} \frac{i_{M\beta}}{i_{M\alpha}}, \tag{35}$$

n_{sr} – the effective stator/rotor turns ratio per phase (voltage ratio).

Generally, it is clear from (30) that, independently of Z_s, Z_r and μ:

$$H_m = \{m = 2pk;\, k = 0, \pm 1, \pm 2, \ldots\}. \tag{36}$$

So, instead of the matrix $\mathbf{Q_{s/r/sr}}$ the Table 1 of harmonic orders balance between ν, ρ, m can be utilised. The triplets synonymously indicate the harmonic inductances $M_{\nu,m}^{s/r/sr}$ prescribed to the given matrix cell.

Table 1. Balance of harmonic orders ν, ρ, m in matrices $\mathbf{M_s^{II}}, \mathbf{M_r^{II}}, \mathbf{M_{sr}^{II}}$

$\rho^{(0)}$	$\rho^{(1)}$	$\rho^{(2)}$	
..., $\pm 9p$, $\pm 3p$,...	...,$-13p$, $-7p$, $-p$, $5p$, $11p$...	...,$-11p$, $-5p$, p, $7p$, $13p$,...	
$m = 6pk$	$m = -2p(1 + 3k)$	$m = 2p(1 + 3k)$	$\nu^{(0)}$ ..., $\pm 9p$, $\pm 3p$,...
$m = 2p(1 + 3k)$	$m = 6pk$	$m = -2p(1 + 3k)$	$\nu^{(1)}$ ..., $-11p$, $-5p$, p, $7p$, $13p$ ...
$m = -2p(1 + 3k)$	$m = 2p(1 + 3k)$	$m = 6pk$	$\nu^{(2)}$ ..., $-13p$, $-7p$, $-p$, $5p$, $11p$, ...

For example we can assume the following sets of harmonic orders:

$$H_\mu = \{-2, 0, 2\}$$
$$H_m = \{-8p, -6p, -4p, -2p, 0, 2p, 4p, 6p, 8p\}$$
$$H_\nu = H_\rho = \{-13p, -11p, -9p, -7p, -5p, -3p, -p, p, 3p, 5p, 7p, 9p, 11p, 13p\}.$$

Thus, for this case, Table 1 takes the form shown below. In this table the harmonic orders $\nu' = \nu / p$, $\rho' = p / p$, $m' = m / p$ are shown.

To formulate the self and mutual inductances of matrices in Equations (24) and (25) the harmonic inductances given by series (27-29) must be known. They are assigned to a specific place of these matrices determined by Table 2. However, for the assumed sets of harmonics H_μ, H_m, H_ν the harmonic inductances are synonymously determined by the mutually dependent numbers μ, ν, m, n. This requirement results from equation (6) under the condition (11). As such, for the given values m and μ resulting from H_m and H_μ, respectively, the possible parameters k and l must be determined by satisfying the equation $m = kZ_s + lZ_r + \mu p$. Hence, the equation $n = lZ_r$ is given for the inductances. From the above it is clear that the numbers k need not be known explicitly. They are hidden in the parameters m.

For the analysed example the determined sets of numbers m', k, l, μ are presented in Table 3 for the three-phase motor with $Z_s = 36$, $Z_r = 24$, $p = 4$.

Table 2. An example of harmonic orders ν', ρ', m' corresponding to Table 1

ρ'	−9	−3	3	9	ρ'	−13	−7	−1	5	11	ρ'	−11	−5	1	7	13
m'	ν'				m'	ν'					m'	ν'				
−6		9	3	−3	−8			9	3	−3	−4		9	3	−3	−9
0	9	3	−3	−9	−2		9	3	−3	−9	2	9	3	−3	−9	
6	3	−3	−9		4	9	3	−3	−9		8	3	−3	−9		
m'	ν'				m'	ν'					m'	ν'				
−4	13	7	1	−5	−6		13	7	1	−5	−8		13	7	1	−5
2	7	1	−5	−11	0	13	7	1	−5	−11	−2	13	7	1	−5	−11
8	1	−5	−11		6	7	1	−5	−11		4	7	1	−5	−11	
m'	ν'				m'	ν'					m'	ν'				
−8		11	5	−1	−4		11	5	−1	−7	−6		11	5	−1	−7
−2	11	5	–1	–7	2	11	5	–1	–7	–13	0	11	5	–1	–7	–13
4	5	–1	–7	−13	8	5	−1	−7	−13		6	5	−1	−7	−13	

Table 3. Sets of numbers m', k, l, μ supplementing Table 2

$m' = m/p$	k	l	μ
−8	−4	5	−2
	−2	2	−2
	0	−1	−2
	2	−4	−2
−6	−4	5	0
	−2	2	0
	0	−1	0
	2	−4	0
−4	−4	5	2
	−2	2	2
	0	−1	2
	2	−4	2
−2	−2	3	−2
	0	0	−2
	2	−3	−2
0	−2	3	0
	0	0	0
	2	−3	0
2	−2	3	2
	0	0	2
	2	−3	2

4	−2	4	−2
	0	1	−2
	2	−2	−2
	4	−5	−2
6	−2	4	0
	0	1	0
	2	−2	0
	4	−5	0
8	−2	4	2
	0	1	2
	2	−2	2
	4	−5	2

It can be observed that the sets of positive and negative numbers are identical for the absolute value. This is the result of applying the Euler's identity.

Both the voltage equation sets for the stator (24) and for the rotor (25) can be transformed into one reference frame *x*-*y* rotating at the angular speed $\omega_x = d\alpha/\mathrm{d}t$ with respect to the axis α of the stationary reference frame α-β. The transformation matrix

$$\mathbf{T}_{\alpha\beta}^{\mathbf{xy}} = \mathrm{diag}[1\ e^{-j\alpha}\ \ e^{j\alpha}] \tag{37}$$

does not change the zero components of stator and rotor voltages and currents.

Denoting the real and imaginary parts of transformed voltage and current vectors by *x* and *y*, respectively, the following relationships are then valid

$$\left.\begin{aligned}
\underline{u}_s &= u_{sx} + ju_{sy} = \underline{u}_s^{(1)} e^{-j\alpha} \\
\underline{u}_r &= u_{rx} + ju_{ry} = n_{sr}\underline{u}_r^{(1)} e^{-j\alpha} \\
\underline{i}_s &= i_{sx} + ji_{sy} = \underline{i}_s^{(1)} e^{-j\alpha} \\
\underline{i}_r &= i_{rx} + ji_{ry} = \tfrac{1}{n_{sr}}\underline{i}_r^{(1)} e^{-j\alpha} \\
i_M &= i_{sx} + i_{rx} = \underline{i}_s + \underline{i}_r \\
i_{ry} &= -i_{sy}
\end{aligned}\right\}. \tag{38}$$

Removing i_{ry} from the set of differential equations the position angle α becomes the state variable together with i_{sx}, i_{sy}, i_{rx} and the rotor speed ω. So, we can obtain the final form of differential equations describing the machine. The differential equations describe now the DC circuit representing the machine.

According to (24) and using (38) the stator voltage equations for the stator and the rotor star connections can be written now in the form presented below.

$$\begin{bmatrix} u_s^{(0)} \\ \underline{u}_s^{(1)} \\ \underline{u}_s^{(2)} \end{bmatrix} = \begin{bmatrix} R_{s0} & \underline{R}_s^* & \underline{R}_s \\ \underline{R}_s & R_{s0} & \underline{R}_s^* \\ \underline{R}_s^* & \underline{R}_s & R_{s0} \end{bmatrix} \begin{bmatrix} 1 & & \\ & e^{j\alpha} & \\ & & e^{-j\alpha} \end{bmatrix} \begin{bmatrix} 0 \\ \underline{i}_s \\ \underline{i}_s^* \end{bmatrix} +$$

$$+ \begin{bmatrix} L_{s0} & \underline{L}_s^* & \underline{L}_s \\ \underline{L}_s & L_{s0} & \underline{L}_s^* \\ \underline{L}_s^* & \underline{L}_s & L_{s0} \end{bmatrix} \frac{\mathrm{d}}{\mathrm{d}t} \begin{bmatrix} 1 & & \\ & e^{j\alpha} & \\ & & e^{-j\alpha} \end{bmatrix} \begin{bmatrix} 0 \\ \underline{i}_s \\ \underline{i}_s^* \end{bmatrix} +$$

$$+ \frac{\mathrm{d}}{\mathrm{d}t} \sum_{\mu,\nu,m,n} 3M_{\nu,m}^{s} \mathbf{Q_s} e^{jn\varphi} e^{-j\mu\alpha} \begin{bmatrix} 1 & & \\ & e^{j\alpha} & \\ & & e^{-j\alpha} \end{bmatrix} \begin{bmatrix} 0 \\ \underline{i}_s \\ \underline{i}_s^* \end{bmatrix} \tag{39}$$

$$+ \frac{\mathrm{d}}{\mathrm{d}t} \sum_{\mu,\nu,m,n} 3M_{\nu,m}^{sr} \mathbf{Q_{sr}} e^{jn\varphi} e^{-j\mu\alpha} \cdot$$

$$\cdot e^{j(\nu+m)\varphi} \begin{bmatrix} 1 & & \\ & e^{-jp\varphi} & \\ & & e^{jp\varphi} \end{bmatrix} \begin{bmatrix} 1 & & \\ & e^{j\alpha} & \\ & & e^{-j\alpha} \end{bmatrix} \begin{bmatrix} 0 \\ \underline{i}_r \\ \underline{i}_r^* \end{bmatrix}.$$

Taking into account that the positive and negative harmonic orders are the same for the absolute value the last two terms of the formula (39) can be written in the form:

$$\frac{\mathrm{d}}{\mathrm{d}t} \sum_{\mathbf{Q_s} \to \mu,\nu,m,n} 3M_{\nu,m}^{s} \begin{bmatrix} e^{\pm jn\varphi} e^{\mp j\mu\alpha} & e^{j(1-\mu)\alpha} e^{jn\varphi} & e^{-j(1-\mu)\alpha} e^{-jn\varphi} \\ e^{\pm jn\varphi} e^{\mp j\mu\alpha} & e^{j(1-\mu)\alpha} e^{jn\varphi} & e^{-j(1-\mu)\alpha} e^{-jn\varphi} \\ e^{\pm jn\varphi} e^{\mp j\mu\alpha} & e^{j(1-\mu)\alpha} e^{jn\varphi} & e^{-j(1-\mu)\alpha} e^{-jn\varphi} \end{bmatrix} \begin{bmatrix} 0 \\ \underline{i}_s \\ \underline{i}_s^* \end{bmatrix} +$$

$$+ \frac{\mathrm{d}}{\mathrm{d}t} \sum_{\mathbf{Q_{sr}} \to \mu,\nu,m,n} 3M_{\nu,m}^{sr} \cdot \tag{40}$$

$$\cdot \begin{bmatrix} e^{\pm jn\varphi} e^{\mp j\mu\alpha} e^{\pm j(\nu+m)\varphi} & e^{j(1-\mu)\alpha} e^{jn\varphi} e^{j(\nu+m-p)\varphi} & e^{-j(1-\mu)\alpha} e^{-jn\varphi} e^{-j(\nu+m-p)\varphi} \\ e^{\pm jn\varphi} e^{\mp j\mu\alpha} e^{\pm j(\nu+m)\varphi} & e^{j(1-\mu)\alpha} e^{jn\varphi} e^{j(\nu+m-p)\varphi} & e^{-j(1-\mu)\alpha} e^{-jn\varphi} e^{-j(\nu+m-p)\varphi} \\ e^{\pm jn\varphi} e^{\mp j\mu\alpha} e^{\pm j(\nu+m)\varphi} & e^{j(1-\mu)\alpha} e^{jn\varphi} e^{j(\nu+m-p)\varphi} & e^{-j(1-\mu)\alpha} e^{-jn\varphi} e^{-j(\nu+m-p)\varphi} \end{bmatrix} \begin{bmatrix} 0 \\ \underline{i}_r \\ \underline{i}_r^* \end{bmatrix}.$$

The above description is valid when for each element of the matrices the relevant harmonics, belonging to the determined sets, are considered.

2.4. The zero sequence voltage

The formula describing the zero sequence voltage results directly from expressions (39), (40):

$$u_s^{(0)} = 2\,\mathrm{Re}\left\{ \underline{R}_s^* \underline{i}_s e^{j\alpha} \right\} + 2\,\mathrm{Re}\left\{ \underline{L}_s^* \frac{\mathrm{d}\underline{i}_s}{\mathrm{d}t} e^{j\alpha} + j\omega_x \underline{L}_s^* \underline{i}_s e^{j\alpha} \right\} +$$

$$+ 2\,\mathrm{Re}\left\{ \frac{\mathrm{d}}{\mathrm{d}t} \sum_{\mu,\nu,m,n} 3M_{\nu,m}^{s} \underline{i}_s e^{j(1-\mu)\alpha} e^{jn\varphi} \right\} + \tag{41}$$

$$+ 2\,\mathrm{Re}\left\{ \frac{\mathrm{d}}{\mathrm{d}t} \sum_{\mu,\nu,m,n} 3M_{\nu,m}^{sr/} \underline{i}_r e^{j(1-\mu)\alpha} e^{jn\varphi} e^{j(\nu+m-p)\varphi} \right\}.$$

Determining the whole derivatives

$$u_s^{(0)} = 2\,\mathrm{Re}\left\{ \underline{R}_s^* \underline{i}_s e^{j\alpha} \right\} + 2\,\mathrm{Re}\left\{ \underline{L}_s^* \frac{\mathrm{d}\underline{i}_s}{\mathrm{d}t} e^{j\alpha} + j\omega_x \underline{L}_s^* \underline{i}_s e^{j\alpha} \right\} +$$

$$+ 6\,\mathrm{Re}\left\{ \sum_{\mu,\nu,m,n} \left(\frac{\partial M_{\nu,m}^{s}}{\partial i_M} \underline{i}_s + \frac{\partial M_{\nu,m}^{sr/}}{\partial i_M} \underline{i}_r e^{j(\nu+m-p)\varphi} \right) \frac{\mathrm{d}i_M}{\mathrm{d}t} e^{j(1-\mu)\alpha} e^{jn\varphi} \right\} +$$

$$+ 6\,\mathrm{Re}\left\{ \sum_{\mu,\nu,m,n} j\{[n\omega + (1-\mu)\omega_x][M_{\nu,m}^{s} \underline{i}_s + M_{\nu,m}^{sr/} \underline{i}_r] + \right. \tag{42}$$

$$\left. + (\nu + m - p)\omega M_{\nu,m}^{sr/} \underline{i}_r e^{j(\nu+m-p)\varphi} \} e^{j(1-\mu)\alpha} e^{jn\varphi} \right\} +$$

$$+ 6\,\mathrm{Re}\left\{ \sum_{\mu,\nu,m,n} \left(M_{\nu,m}^{s} \frac{\mathrm{d}\underline{i}_s}{\mathrm{d}t} + M_{\nu,m}^{sr/} \frac{\mathrm{d}\underline{i}_r}{\mathrm{d}t} e^{j(\nu+m-p)\varphi} \right) e^{j(1-\mu)\alpha} e^{jn\varphi} \right\}.$$

The above expression takes into account the ratio n_{sr} that changes the value of $M_{\nu,m}^{sr}$ yielding $M_{\nu,m}^{sr/} = n_{sr} M_{\nu,m}^{sr}$. Additionally, $\omega = \mathrm{d}\varphi/\mathrm{d}t$ – the rotor speed, $\omega_x = \mathrm{d}\alpha/\mathrm{d}t$ – the reference frame speed.

For the steady state: $\alpha = \omega_x t = \omega_s t$, $\varphi = \omega t$, $\mathrm{d}tM/\mathrm{d}t = 0$, $\mathrm{d}t_s/\mathrm{d}t = 0$, where $\omega_s = 2\pi f_s$ – angular frequency of mono-harmonic supplying voltages. At the rotor's one broken phase the steady state phase currents assume the values: $i_K^{/} = I_r^{/} \sin(n_1 s\omega_s t)$, $i_L^{/} = -i_K^{/}$, , $i_M^{/} = 0$ (n_1 = 1, 2, 3,... , s – motor slip, $I_r^{/} = Ir/n_{sr}$). Thus, the rotor current vector takes the following form in the *x*-*y* reference frame:

$$\underline{i}_r = \frac{I_r^{/}}{2} (e^{j(n_1-1)s\omega_s t} - e^{-j(n_1+1)s\omega_s t}). \tag{43}$$

Hence, omitting derivatives of currents, the zero sequence voltage $u_s^{(0)}$ takes the simplified form containing only the rotational components:

$$u_s^{(0)} = 2\,\mathrm{Re}\left\{ \underline{R}_s^* \underline{i}_s e^{j\omega_s t} \right\} + 2\,\mathrm{Re}\left\{ j\omega_s \underline{L}_s^* \underline{i}_s e^{j\omega_s t} \right\} +$$

$$+ 6\,\mathrm{Re}\left\{ \sum_{\mu,\nu,m,n} j\{[n\omega + (1-\mu)\omega_s] \cdot [(M_{\nu,m}^{s} \underline{i}_s + M_{\nu,m}^{sr/} \frac{I_r^{/}}{2} (e^{j(n_1-1)s\omega_s t} - e^{-j(n_1+1)s\omega_s t})] + \right. \tag{44}$$

$$\left. + (\nu + m - p)\omega M_{\nu,m}^{sr/} \frac{I_r^{/}}{2} (e^{j(n_1-1)s\omega_s t} - e^{-j(n_1+1)s\omega_s t}) e^{j(\nu+m-p)\omega t} \} e^{j(1-\mu)\omega_s t} e^{jn\omega t} \right\}.$$

These components are the alternating waveforms of frequencies specific for the symmetry condition and indicating the asymmetry. More detailed analysis allows for additional components of the zero voltage to be interpreted. For the rotor asymmetry this approach has been sufficient.

- Symmetry

There are two series

$$\omega_1 = (1-\mu)\omega_s + n\omega,$$

$$\omega_2 = \omega_1 + (\nu + m - p)\omega.$$

Introducing:

$$\omega = \frac{\omega_s}{p}(1-s), \quad \mu = -10, -6, -2, 0, 2, 6, 10, \quad n = -lZ_r, \quad \nu + m = -\rho = (1+6k)p$$

the following frequencies can be distinguished:

$$f_{s1} = f_s \left| (1-\mu) - \frac{lZ_r}{p}(1-s) \right|, \tag{45}$$

$$f_{s2} = f_s \left| (1-\mu) + (-\frac{lZ_r}{p} + 2 + 6k)(1-s) \right|, \tag{46}$$

$$l = 0, \pm 1, \pm 2, \ldots; k = 0, \pm 1, \pm 2, \ldots$$

- Asymmetry

The relevant spectrum contains frequencies f_{s1} (45), f_{s2} (46) and additionally the frequencies caused by the asymmetry:

$$f_{s3} = f_{s1} - (n_1 + 1)sf_s \;|_{n_1=1} = f_{s1} - 2sf_s, \tag{47}$$

$$f_{s4} = f_{s2} - (n_1 + 1)sf_s \;|_{n_1=1} = f_{s2} - 2sf_s, \tag{48}$$

$$f_{s5} = f_s. \tag{49}$$

3. Laboratory tests

The influence of rotor asymmetry on the zero sequence voltage was tested using the slip-ring induction motor SZUDe48a. The ratings are: P_N = 2.2 kW, $U_{s\text{-}sN}$ = 380 V (Y), I_{sN} = 7.6 A, f_{sN} = 50 Hz, n_N = 690 rev/min, η_N = 0.68, $U_{r\text{-}rN}$ = 62 V (Y), I_{rN} = 24.5 A. Stator parameters: m_s = 3 (number of phases), Z_s = 36, Z_r = 24, p = 4, $q_s = Z_s/(2m_s p)$ = 1.5.

The motor was supplied with the 3-phase mains of the r.m.s. value equal to 400 V. The supplying voltages were distorted with respect to pure sinusoid with higher harmonics of the orders: 3 (6.85 V), 5 (3.84 V), 7 (1.01 V), 9 (0.892 V), 11 (1.413 V) 15 (1 V). The steady state waveforms are shown in Figure 3.

The influence of rotor asymmetry was analyzed on the background of symmetrical operation. The asymmetry was performed as the failure of the rotor phase *M*. Results of measurements are shown in Figures 3 and 4 for the motor loaded with the approximately rated torque value. Harmonic bars of u_n observed at symmetrical and asymmetrical operation can be predicted using the formulae (45) – (49).

It seems the theoretically predicted harmonic components of $u_n = u_s^{(0)}/\sqrt{3}$, specific for the symmetrical operation, appear in the real machine. The harmonic bars for f_{s1} in Figure 5a are caused by the magnetic saturation. Additionally, it is visible by the bar at f_{s5} = 50 Hz indicating an asymmetry in the stator. This can be caused by an asymmetrical supply, internal

asymmetry of the stator circuit or the anisotropy. For the studied motor the two former reasons are most likely contributors.

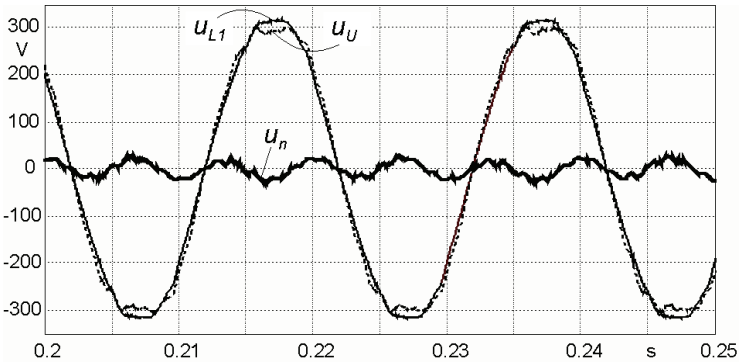

Fig. 3. Measured voltages in the system from Fig. 1

The rotor asymmetry is synonymously indicated by the bar f_{s5} in Figure 5b. Additionally, for currents i_U and i_K the characteristic bars have been shown for frequencies in square boxes. The distortion of supply voltages with higher harmonics does not influence the neutral voltage waveform u_n.

In the figures only the greatest bars were analyzed. They can be easily measured and observed in the linear scale.

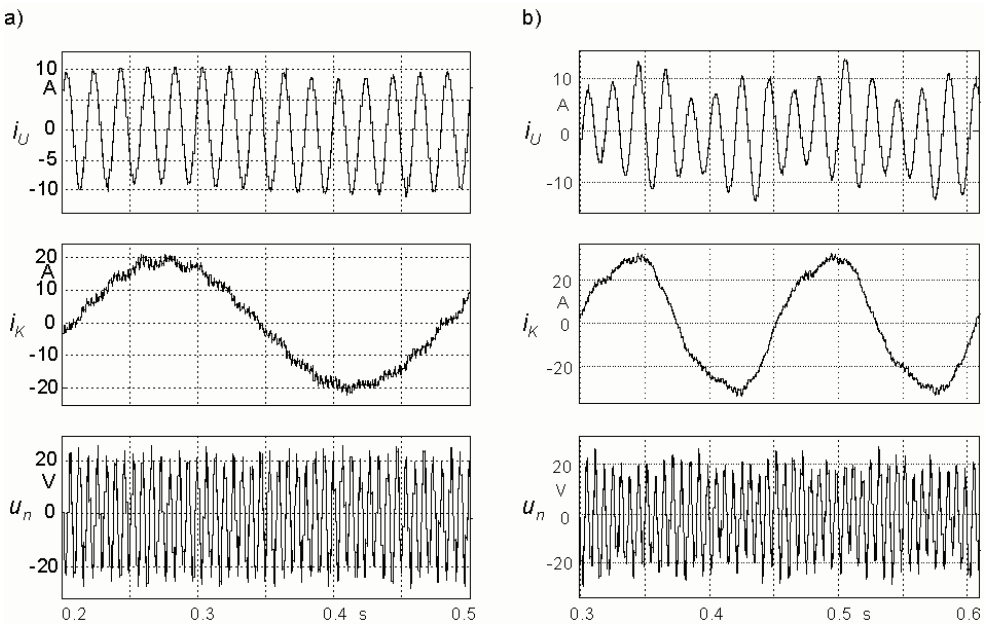

Fig. 4. Measured waveforms of stator and rotor phase currents and the neutral voltage: a) symmetry at the slip $s = 0.0726$, b) asymmetry at $s = 0.1277$

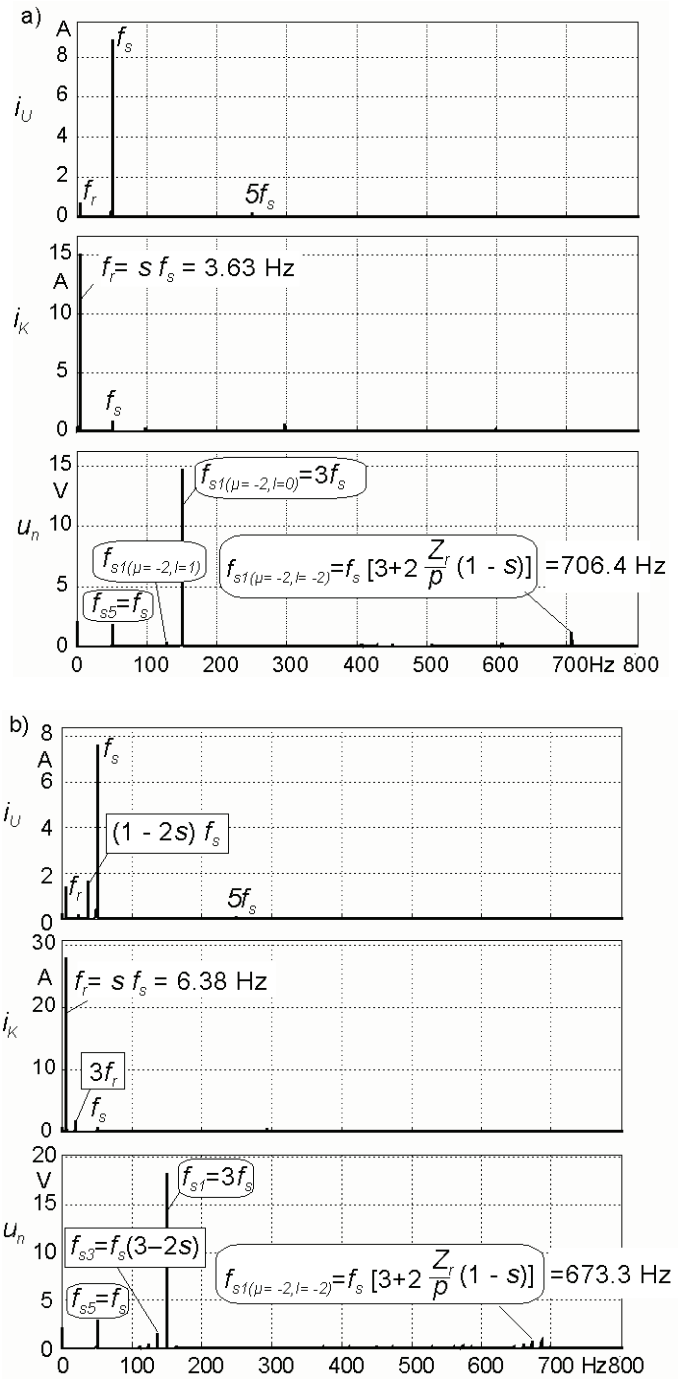

Fig. 5. Spectra of the waveforms: a) from Fig. 4a, b) from Fig. 4b

4. Conclusions

Magnetic saturation of induction motor generates new signals of the neutral voltage indicating the presence of asymmetry of the rotor circuit. This is beneficial only for the star connected stator winding. For the delta connection the zero sequence stator current could be taken into account. Other damages like eccentrically rotating rotors can be detected using this method as well. Distortions of supplying voltages influence the neutral voltage u_n in a low degree. The currents and phase voltages are influenced more. So, this method could be applied for fault detection of induction motors supplied by power electronic units.

Particularly, this can be valid when the motor is supplied with a current source inverter or the current controlled voltage source inverter. In such a case the stator current is forced by the control system and the spectral response is quite different than using the voltage forced operation. So, the signals indicating motor faults should be searched for in voltage signals and, among them, the zero sequence voltage.

References

[1] Bellini A., Filippetti F., Franceschini G. et al., *Quantitative evaluation of induction motor broken bars by means of electrical signature analysis*. IEEE Trans. on Industry Applications 37(5): 1248-1255 (2001).

[2] Dorrell D.G., Thomson W.T., Roach S., *Analysis of airgap flux, current, and vibration signals as a function of the combination of static and dynamic airgap eccentricity in 3-phase induction motors*. IEEE Trans. on Industry Applications 33(1): 24-34 (1997).

[3] Drozdowski P., *Saturation and space harmonics in a star and delta connected squirrel-cage induction motor*. Int. Conf. on Electr. Machines ICEM'94, Paris (France) 3: 93-98 (1994).

[4] Drozdowski P., Petryna J., Weinreb K., *Interaction of electric, magnetic and* mechanical *effects in induction motors under diagnostic demands*. Zeszyty Problemowe BOBRME Katowice 54: 109-116 (1997) (in Polish).

[5] Drozdowski P., Duda A., *Computer analysis of saturated cage induction machine using Sim-PowerSystems of Simulink*. Technical Transactions (Czasopismo techniczne), Electrical Engineering 1-E/2012. Wyd. Politechniki Krakowskiej, Kraków, pp. 33-48 (2012).

[6] Heller B., Hamata V., *Harmonic field effects in induction machines*. Academia Publishing House of the Czechoslovak Academy of Sciences, Prague (1977).

[7] Kowalski Cz., *Monitoring and diagnosis of induction motors faults using neural* networks. Prace Naukowe IMNiPE Politechniki Wrocławskiej 57, Monography 18, Wrocław (2005) (in Polish).

[8] Nandi S., *Modeling of induction machines including stator and rotor slot effects*. IEEE Trans. on Industry Applications 40(4): 1058-1065 (2004).

[9] Nandi S., *A detailed model of induction machines with saturation extendable for fault analysis*. IEEE Trans. on Industry Applications 40(5): 1302-1309 (2004).

[10] Oumaamar M.E.K., Babaa F., Khezzar A., Boucherma M., *Diagnostics of Broken Rotor Bars in Induction Machines Using the Neutral Voltage*. Proc. of ICEM. 2-5.09.2006. Chania. Crete Island, Greece (2006).

[11] Sobczyk T.J., Drozdowski P., *Inductances of electrical machine winding with a nonuniform air-gap.* Archiv für Elektrotechnik 76: 213-218 (1993).

[12] Sobczyk T.J., Weinreb K., Węgiel T., Sułowicz M., *Influence of Stator and Rotor Slotting on Quantitative Prediction of Induction Motor Rotor Eccentricity*. Proc. of SDEMPED. 1-3.09.2001. Gorizia, Italy pp. 429-434.

[13] Sobczyk T., Weinreb K., Sułowicz M. et al., *Slot Harmonics in Cage Motors due to Saturation of a Main Magnetic Circuit*. COMPEL 25(1): 128-139 (2006).
[14] Toliyat H.A., Lipo T.A., *Transient Analysis of Cage Induction Machines Under Stator, Rotor Bar and End Ring Faults*. IEEE Trans. on Energy Conversion 10(2): 241-247 (1995).
[15] Weinreb K., Węgiel T., Sułowicz M., *Influence of the Main Magnetic Circuit Saturation on Stator Current Spectrum for a Cage Induction Motor with Rotor Asymmetry*. Technical Transactions (Czasopismo techniczne). Z. 6-E/2006, Wyd. Politechniki Krakowskiej, Kraków, pp. 65-76 (2006).
[16] Węgiel T., Weinreb K., Sułowicz M., *Main inductances of induction motor for diagnostically specialized mathematical models.* Archives of Electrical Engineering 59(1-2): 51-66 (2010).